ACS APPLIED MATERIALS & INTERFACES

Research Article

www.acsami.org

Aqueous-Phase Linker-Assisted Attachment of Cysteinate(2$^-$)-Capped CdSe Quantum Dots to TiO_2 for Quantum Dot-Sensitized Solar Cells

Kathleen M. Coughlin, Jeremy S. Nevins, and David F. Watson*

Department of Chemistry, University at Buffalo, The State University of New York Buffalo, New York 14260-3000, United States

Supporting Information

ABSTRACT: We have synthesized water-dispersible cysteinate(2$^-$)-capped CdSe nanocrystals and attached them to TiO_2 using one-step linker-assisted assembly. Room-temperature syntheses yielded CdSe magic-sized clusters (MSCs) exhibiting a narrow and intense first excitonic absorption band centered at 422 nm. Syntheses at 80 °C yielded regular CdSe quantum dots (RQDs) with broader and red-shifted first excitonic absorption bands. Cysteinate(2$^-$)-capped CdSe MSCs and RQDs adsorbed to bare nanocrystalline TiO_2 films from aqueous dispersions. CdSe-functionalized TiO_2 films were incorporated into working electrodes of quantum dot-sensitized solar cells (QDSSCs). Short-circuit photocurrent action spectra of QDSSCs corresponded closely to absorptance spectra of CdSe-functionalized TiO_2 films. Power-conversion efficiencies were (0.43 ± 0.04)% for MSC-functionalized TiO_2 and (0.83 ± 0.11)% for RQD-functionalized TiO_2. Absorbed photon-to-current efficiencies under white-light illumination were approximately 0.3 for both MSC- and RQD-based QDSSCs, despite the significant differences in the electronic properties of MSCs and RQDs. Cysteinate(2$^-$) is an attractive capping group and ligand, as it engenders water-dispersibility of CdSe nanocrystals with a range of photophysical properties, enables facile all-aqueous linker-assisted attachment of nanocrystals to TiO_2, and promotes efficient interfacial charge transfer.

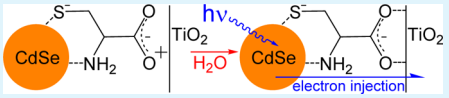

KEYWORDS: *linker-assisted assembly, quantum dot-sensitized solar cell, cysteine, cadmium selenide, magic-sized clusters, electron injection*

INTRODUCTION

Semiconductor quantum dots (QDs) are intriguing light-harvesting materials for solar energy conversion, due to their size-dependent bandgaps and band-edge potentials, their large oscillator strengths, the possibility of multiexciton generation, and the potential role of surface-localized trap states in charge- and energy-transfer processes.[1−4] QD-sensitized solar cells (QDSSCs) and photocatalysts are promising constructs for exploiting these properties.[1,2,5−8] The sensitization mechanism involves transfer of charge carriers from photoexcited QDs to semiconductor substrates.

Several approaches have been explored for placing QDs onto surfaces of semiconductors. In situ synthetic methods, such as successive ionic layer adsorption and reaction (SILAR) and chemical bath deposition, lead to high surface coverages of QDs and yield QDSSCs with power-conversion efficiencies of up to 5.4%.[9−13] However, the post-synthesis attachment of QDs to surfaces via either direct attachment, in which QDs are deposited onto bare substrates, or linker-assisted assembly, in which QDs are tethered to substrates via bifunctional ligands, affords better control over the size and electronic properties of QDs.[14−18] Electron-injection kinetics are sensitive to the deposition mode. Reported rate constants for electron injection from QDs to TiO_2 at interfaces prepared by direct attachment are 1.5−10-fold greater than at interfaces prepared by linker-assisted assembly, probably due to the decreased distance and increased electronic coupling between QDs and TiO_2.[19,20] Under certain conditions, direct or linker-assisted attachment can yield agglomerates of QDs on TiO_2.[15,17,19−22] Agglomeration has been shown to decrease the rate constant of electron injection and the photocurrent efficiencies of QDSSCs.[17,19,21] We are intrigued by linker-assisted assembly because the structure and properties of linkers can be utilized to tune the distance and electronic coupling between QDs and semiconductor substrates, the interfacial charge distribution, and the rates and efficiencies of charge-transfer processes.[14,19,23−25]

In one notable example, Mora-Seró and coworkers reported greater rate constants of electron injection, incident photon-to-current efficiencies (IPCEs), and power-conversion efficiencies for QDSSCs utilizing cysteine as the molecular linker than for QDSSCs with analogous nonaminated linkers.[19,26] They attributed the effects to a decrease of the QD−TiO_2 distance or the formation of a surface dipole that stabilizes the charge-separated state resulting from electron injection.[19,26] Similarly, Margraf et al. reported that the adsorption of zwitterionic cysteine to TiO_2 yields a surface dipole that promotes electron injection and hinders charge recombination, thereby increasing the power-conversion efficiencies of QDSSCs.[27] Both groups assembled QD−cysteine−TiO_2 interfaces by first adsorbing cysteine to TiO_2, then attaching organic-dispersible CdSe QDs to cysteine-functionalized TiO_2 films. Surface-attachment presumably involved the displacement of native capping groups

Received: June 11, 2013
Accepted: August 12, 2013
Published: August 12, 2013

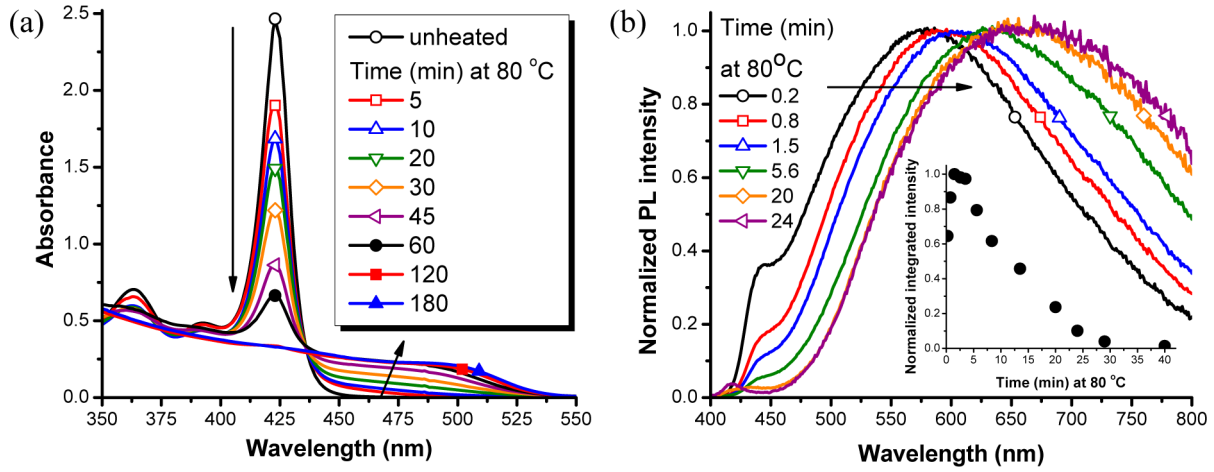

Figure 1. Absorption spectra (a) and normalized photoluminescence (PL) spectra (b) of aqueous dispersions of cysteinate(2^-)-capped CdSe QDs as a function of time that CdSe reaction mixtures were heated at 80 °C. (inset) Integrated emission intensity as a function of reaction time. Arrows indicate spectral changes with reaction time.

of QDs by thiols and/or amines of TiO_2-adsorbed cysteine. This approach to linker-assisted assembly utilizes well-established syntheses of organic-dispersible QDs, enabling facile control of size and optical properties. However, linkers must be adsorbed to surfaces of both QDs and TiO_2 in two separate reactions, and some native capping groups of QDs must be removed or displaced by linkers. The affinity of QDs for linker-functionalized surfaces, as well as the morphology of QD-functionalized nanocrystalline TiO_2 thin films prepared by this route, have been shown to vary greatly with solvation and the extent of postsynthesis washing of QDs.[20−22]

In an alternative approach to linker-assisted assembly, we attached water-dispersible CdSe QDs functionalized with carboxylate-terminated capping groups directly to bare TiO_2 films.[28] We measured enhanced electron injection and longer-lived charge separation with cysteinate(2^-) as linker than with non-aminated ligands. These effects translated into increased absorbed photon-to-current efficiencies (APCEs) and power-conversion efficiencies of QDSSCs. Our all-aqueous linker-assisted assembly is streamlined and simplified, in that it utilizes native capping groups of as-synthesized QDs as linkers, involves only one surface-adsorption reaction, and is not plagued by complications associated with solvation and post-synthesis washing. However, our aqueous dispersions of cysteinate(2^-)-capped CdSe QDs, which we synthesized following the method of Park and co-workers,[29,30] consisted of highly quantum-confined, probably "magic-sized", nanocrystals with diameters less than 2 nm.[28,31] Their absorption onsets were approximately 475 nm, and their absorption spectra exhibited narrow first excitonic transitions centered at 422 nm. Thus, these magic-sized clusters, hereafter referred to as CdSe MSCs, were inefficient harvesters of the solar spectrum and impractical for applications in QDSSCs. In addition, the experimental data did not enable us to determine whether their enhanced electron-injection reactivity and photoelectrochemical performance arose from properties of cysteinate(2^-) or from the improved electronic coupling and/or increased driving force for electron injection from the highly-energetic conduction band-edge and electron-trap states of the MSCs.[28]

In this manuscript, we report the synthesis and photophysical characterization of larger water-dispersible cysteinate(2^-)-capped CdSe QDs with lower-energy absorption onsets, as well as the sensitization of TiO_2 with these QDs. The photoelectrochemical performance of QDSSCs incorporating these larger CdSe QDs was comparable to or better than that of QDSSCs incorporating the CdSe MSCs, suggesting that properties of cysteinate(2^-), rather than MSCs, facilitated efficient electron injection and charge separation. Therefore, cysteinate(2^-) is an attractive linker, and the aqueous linker-assisted assembly chemistry reported herein is a simple and generalizable route for preparing QD−linker−TiO_2 interfaces with tunable light-harvesting properties and desirable photo-induced charge-transfer reactivity.

EXPERIMENTAL SECTION

Materials and Instrumentation. Commercially-available reagents and their sources are as follows: L-cysteine, sodium sulfite, titanium(IV) tetraisopropoxide, lithium iodide, 4-*tert*-butylpyridine, and guanidinium isothiocyanate (Aldrich); selenium, cadmium sulfate octahydrate, sulfur, bis(acetylacetonato)diisopropoxytitanium(IV), and lead foil (99+%, 1.6 mm thick) (Alfa Aesar); 1-methyl-3-propylimidazolium iodide (Fluka); acetonitrile, iodine, and 2-propanol (Fisher); sodium sulfide nonahydrate and sodium hydroxide (JT Baker); nitric acid (EMD); ruthenium 535 (N3 dye) (Solaronix). Reagents were used without further purification. Glass slides coated with fluorine-doped tin oxide (FTO) were generously provided by Pilkington. UV/vis absorption spectra were acquired using an Agilent 8453 diode array spectrophotometer. Photoluminescence spectra were acquired with a Varian Cary Eclipse fluorimeter.

Synthesis of CdSe QDs. Cysteinate(2^-)-capped CdSe MSCs were synthesized from an aqueous reaction mixture containing cadmium sulfate, sodium selenosulfate, and cysteinate(2^-) at pH 12.5-13.0, as described previously.[28,31] To accelerate particle growth and promote the formation of larger cysteinate(2^-)-capped CdSe QDs, we heated reaction mixtures. In a typical synthesis, the selenide precursor was prepared by combining Se (0.17 g, 2.0 mmol) and Na_2SO_3 (0.80 g, 6.0 mmol) in deionized water (diH_2O) (42 mL) and refluxing for 12−16 h. The cadmium precursor was a 53-mL solution of cysteine (160 mM) and $CdSO_4{\cdot}8H_2O$ (42 mM in Cd^{2+}) in diH_2O at pH 12.5−13.0. After 30 min of stirring at room temperature, the cadmium precursor was heated to 80 °C. An aliquot (23 mL) of the hot, refluxing selenide precursor solution was added to the cadmium precursor solution, and the reaction mixture was stirred at constant temperature of 80 °C for a maximum of 2−3 h until the desired absorption spectrum was attained. Reactions were quenched by addition of 30 mL of 2-propanol to 10 mL of reaction mixture to induce flocculation of CdSe QDs. CdSe QDs were isolated by centrifugation and decanting. The

resulting pellet was redispersed into diH_2O (5 mL) for spectral analysis and attachment to TiO_2.

Linker-Assisted Attachment of QDs to Nanocrystalline TiO_2 Films. Nanocrystalline anatase TiO_2 films were deposited onto glass slides (for absorption spectral characterization) or FTO-coated glass slides (for photoelectrochemical measurements) as described previously.[32,33] FTO-coated glass slides were first coated with a dense blocking layer of TiO_2 following the method of Tachibana et al.[34] TiO_2 films were functionalized by immersion in aqueous dispersions of cysteinate(2^-)-capped CdSe QDs or MSCs, which had been flocculated from their original reaction mixtures and redispersed into diH_2O, for 4−16 h.

Photoelectrochemistry. Short-circuit photocurrent action spectra and photocurrent-photovoltage data were acquired using instrumentation[35] and methods[28] described previously. The ruthenium(II) dye N3 was used as a reference sensitizer.[36] Two-electrode cells consisted of a CdSe- or N3-functionalized TiO_2-on-FTO working electrode and either a PbS counter electrode for QDSSCs or a Pt-coated FTO counter electrode for N3-sensitized cells. PbS electrodes were prepared as described by Tachan et al.[37] An aqueous polysulfide electrolyte containing sodium sulfide (1 M), sulfur (0.65 M), and sodium hydroxide (0.1 M) was used for QDSSCs. The electrolyte for N3-sensitized cells consisted of iodine (0.05 M), lithium iodide (0.1 M), 1-methyl-3-propylimidazolium iodide (0.6 M), 4-*tert*-butylpyridine (0.6 M), and guanidinium isothiocyanate (0.1 M) in acetonitrile. The backside of the working electrode was illuminated with a 0.47-cm^2 beam. Monochromatic spectral irradiances ranged from 3.2×10^{-3} to 5.7×10^{-3} mW cm^{-2} nm^{-1}; the integrated irradiance was 1.2 mW cm^{-2}. The configuration of electrochemical cells was identical for photocurrent−photovoltage measurements. Data were acquired using the full output of a 75-W Xe lamp (Newport Photomax). The irradiance was 56 mW cm^{-2}.

RESULTS AND DISCUSSION

Photophysical Properties of CdSe QDs. When CdSe QD-containing reaction mixtures were heated at 80 °C, the absorbance of the first excitonic absorption band at 422 nm decreased significantly; concomitantly, a broader and red-shifted absorption band developed (Figure 1a). After 3 h, the new band exhibited a maximum of 487 nm and an onset of approximately 550 nm, and the narrow 422-nm excitonic band of MSCs had diminished almost completely. The broader and less intense lowest-energy absorption band of the heated samples is typical of QDs larger than MSCs.[38−41] Thus, the absorption spectral changes suggest that elevating the temperature of reaction mixtures accelerated particle growth, leading to an increase of the average size of CdSe QDs within the reaction mixture. By flocculating QDs through the addition of 2-propanol, in which the cysteinate(2^-)-capped QDs are not dispersible, we isolated the larger QDs rather than the more thermodynamically stable MSCs that predominate in equilibrated reaction mixtures at room temperature.[28,31,42] We hereafter refer to the larger QDs with red-shifted absorption spectra as "regular" CdSe QDs or RQDs, to distinguish them from the MSCs.

Photoluminescence spectra of the CdSe MSCs synthesized at room temperature exhibited a narrow band-edge emission band centered at 432 nm and a more intense and broader trap-state emission band centered at 515 nm.[28] When reaction mixtures were heated at 80 °C, the band-edge emission intensity decreased rapidly and the trap-state emission band red-shifted and diminished (Figure 1b). After 20 min of heating, the maximum of the trap-state emission band had shifted to approximately 655 nm. Emission was completely quenched after 1 h of heating at 80 °C. The decreased contribution of band-edge emission from RQDs relative to MSCs indicates that fewer band-edge electrons in RQDs were involved in radiative recombination. Similarly, the red-shift of trap-state emission for RQDs relative to MSCs indicates that electrons were, on average, trapped more deeply in RQDs than MSCs. This shift of excited-state electrons in RQDs, on average, to lower energies than excited-state electrons in MSCs, suggests that the average driving force for electron injection into TiO_2 was probably lower for RQDs than MSCs.

Adsorption of CdSe MSCs and RQDs to TiO_2. Immersion of TiO_2 films into aqueous dispersions of MSCs and/or RQDs, which had been removed from the original reaction mixtures and redispersed into diH_2O, caused the films to turn yellow or orange due to attachment of CdSe. The lowest-energy excitonic absorption bands of CdSe MSCs and RQDs were unshifted upon attachment to TiO_2 (Figure 2).

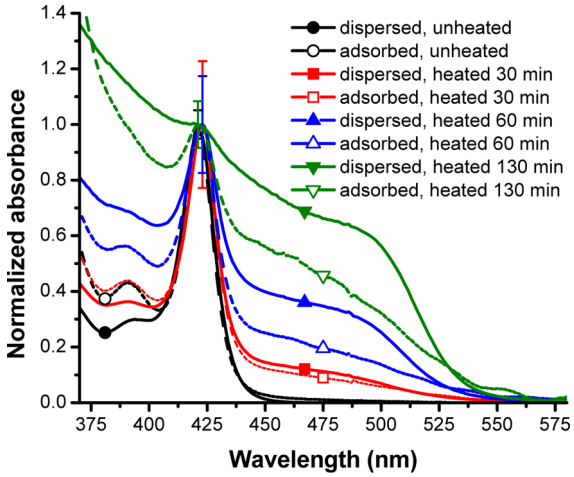

Figure 2. Normalized absorption spectra of dispersions of CdSe QDs (solid lines) and of TiO_2 films functionalized with QDs (dashed lines) as a function of time that CdSe reaction mixtures were heated at 80 °C. Error bars represent +/− one standard deviation from the average absorbance of two films at the first excitonic absorption maximum of MSCs.

However, for TiO_2 films functionalized from mixed dispersions of MSCs and RQDs, the absorbance at 422 nm, corresponding the first excitonic maximum of MSCs, increased relative to the absorbance at the first excitonic maximum of RQDs, suggesting that MSCs adsorbed preferentially to TiO_2 (Figure 2). Despite this apparent difference in surface-adduct formation constants of MSCs and RQDs, the absorption spectra of CdSe-functionalized TiO_2 films could be adjusted significantly by varying the relative amounts of MSCs and RQDs in the dispersions from which CdSe was adsorbed.

Photoelectrochemical Characterization of QDSSCs. To compare the performance of MSCs and RQDs as sensitizers, we functionalized TiO_2 films with CdSe from three dispersions containing different relative amounts of MSCs and RQDs. One dispersion consisted primarily of CdSe MSCs, which were synthesized at room temperature then flocculated and redispersed into diH_2O. The second and third dispersions consisted of mixtures of CdSe MSCs and RQDs, which had been isolated from reaction mixtures heated at 80 °C for 30 and 90 min, respectively. Average absorption spectra of the corresponding CdSe-functionalized TiO_2 films are shown in Figure 3. The spectrum of TiO_2 films functionalized with CdSe from the room-temperature reaction mixture exhibits a narrow

dx.doi.org/10.1021/am402219e | ACS Appl. Mater. Interfaces 2013, 5, 8649−8654

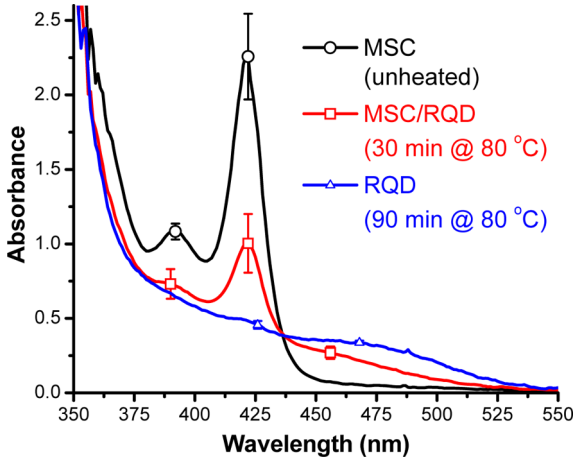

Figure 3. Absorption spectra of MSC-, MSC/RQD-, and RQD-functionalized TiO_2 films. Error bars represent +/− one standard deviation from the average absorbances of 3-5 films at or near excitonic absorption maxima.

first excitonic absorption band centered at 422 nm and negligible longer-wavelength absorption. These films are hereafter referred to as MSC-functionalized TiO_2. The spectra of TiO_2 films functionalized with CdSe from the reaction mixture at 80 °C exhibit diminished 422-nm excitonic absorption bands and significant absorption beyond 450 nm. Thus, these TiO_2 films were functionalized with mixtures of MSCs and RQDs. We were unable to estimate relative mole fractions of MSCs and RQDs on these films, due to the size-dependent shifts and unknown molar absorption coefficients of the first excitonic absorption band of RQDs. However, the CdSe sample that reacted at 80 °C for 30 min clearly contains fewer RQDs and more MSCs than the sample that reacted at 80 °C for 90 min. TiO_2 films functionalized with these 30- and 90-min CdSe samples are hereafter referred to as MSC/RQD-functionalized TiO_2 and RQD-functionalized TiO_2, respectively.

Short-circuit photocurrent action spectra (IPCE vs wavelength) were acquired for QDSSCs incorporating MSC-, MSC/RQD-, and RQD-functionalized TiO_2 films as working electrodes. We measured photocurrent action spectra for N3-sensitized TiO_2 films as a reference and obtained an average IPCE value of 0.59 ± 0.03 at 536 nm (Figure S1 in the Supporting Information), corresponding to approximately three-fourths of reported literature values.[36,43] Photocurrent action spectra of our QDSSCs coincided closely with absorptance spectra and extended to wavelengths much longer than the absorption onset of TiO_2 (Figure 4). (Absorptance equals the fraction of photons absorbed, or one minus transmittance.) Thus, the MSCs and RQDs sensitized TiO_2. RQD-functionalized TiO_2 electrodes exhibited the highest average monochromatic IPCE of 0.27 ± 0.03 at 460 nm, near the maximum of the long-wavelength excitonic absorption band. The maximum monochromatic IPCEs of MSC- and MSC/RQD-functionalized TiO_2 electrodes were 0.19 ± 0.01 and 0.2 ± 0.1, respectively. The relatively large standard deviation of IPCE for MSC-functionalized TiO_2 arose from degradation of MSCs upon exposure to the electrolyte solution, which gave rise to shifts of absorption and photocurrent action spectra.[28] Values of monochromatic absorbed photon-to-current efficiency (APCE), or IPCE divided by absorptance, were approximately 0.2 at the excitonic maximum of MSCs and

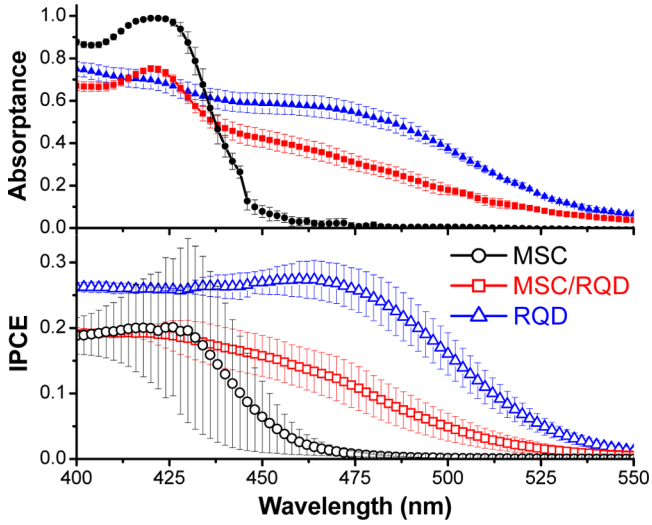

Figure 4. Short-circuit photocurrent action spectra (open symbols, lower graph) and absorptance spectra (closed symbols, upper graph) for QDSSCs with MSC-, MSC/RQD-, and RQD-functionalized TiO_2 electrodes. Error bars represent +/− one standard deviation from the average of measurements on 3−5 films; one absorptance spectrum and two photocurrent action spectra were acquired per film.

approximately 0.35−0.4 at the lower-energy excitonic maximum of RQDs (Figure S2 in the Supporting Information).

Photocurrent density (J) was measured as a function of photovoltage (V) for QDSSCs under white-light illumination at 56 mW cm^{-2}. $J-V$ data for N3-sensitized TiO_2 as a reference are shown in Figure S3 in the Supporting Information. We measured an average global energy-conversion efficiency (η) of (4.4 ± 0.6)% for N3-sensitized solar cells, corresponding to approximately 45% of reported η values with simulated AM 1.5 solar illumination.[36] Representative $J-V$ data for QDSSCs are shown in Figure 5, and averaged parameters are presented in Table 1. Our measured fill factors of 0.45−0.5 are typical of QDSSCs with photoanodes prepared by post-synthesis deposition of QDs,[18,19,26,44,45] approximately 5−20% lower than those of the record-setting QDSSCs recently reported by Zhong and co-workers,[46−48] and 25−45% lower than fill factors of fully optimized dye-sensitized solar cells.[43,49] The relatively

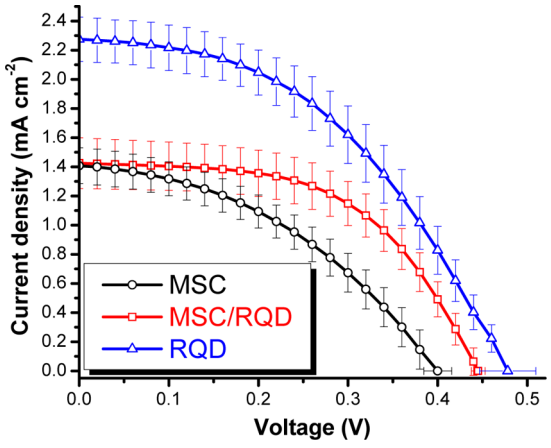

Figure 5. $J-V$ data for QDSSCs with MSC-, MSC/RQD-, and RQD-functionalized TiO_2 electrodes. Error bars represent +/− one standard deviation from the average of a total of 12−24 measurements on 6−12 different working electrodes.

dx.doi.org/10.1021/am402219e | ACS Appl. Mater. Interfaces 2013, 5, 8649−8654

Table 1. Summary of Photocurrent−Photovoltage data

sensitizer(s)	J_{sc} (mA cm^{-2})^{a,b}	V_{oc} (V)^{a,b}	ff^{a,c}	η (%)^{a,b}	$q_{p,abs}/10^{16}$ (s^{-1} cm^{-2})^{a,b}	APCE$_{WL}$^{a,b}
MSC	1.4 ± 0.1	0.40 ± 0.02	0.45 ± 0.04	0.43 ± 0.04	3.0 ± 0.2	0.29 ± 0.03
MSC/RQD	1.4 ± 0.2	0.45 ± 0.01	0.54 ± 0.02	0.58 ± 0.07	3.8 ± 0.5	0.24 ± 0.04
RQD	2.3 ± 0.3	0.48 ± 0.03	0.46 ± 0.05	0.83 ± 0.11	4.4 ± 0.2	0.32 ± 0.03

[a]Standard deviations relative to average of 12−24 measurements on 6−12 working electrodes. [b]Abbreviation defined in text. [c]ff = fill factor.

low fill factors of QDSSCs have been attributed to high charge-transfer resistance at the counter electrode−electrolyte interface.[6,18,37,44,50] The measured value of η for QDSSCs with MSC-functionalized TiO_2 ((0.43 ± 0.04)%) was nearly identical to our previously-reported value.[28] QDSSCs with RQD-functionalized TiO_2 electrodes outperformed those with MSC-functionalized TiO_2 electrodes. Our highest value of η was (0.83 ± 0.11)% for QDSSCs incorporating RQD-functionalized TiO_2. The nearly two-fold increase of η relative to MSC-functionalized TiO_2 arose from an approximately 65% increase of short-circuit photocurrent density (J_{sc}) and an approximately 20% increase of open-circuit photovoltage (V_{oc}). Average values of η and V_{oc} for MSC/RQD-functionalized TiO_2 were intermediate between those of RQD- and MSC-functionalized TiO_2. Our η values of 0.4−1% are similar to many reported values for QDSSCs prepared by linker-assisted assembly.[19,26,44,45] However, they pale in comparison to reported η values of 3.8% to 5.4% for QDSSCs prepared by CBD or SILAR,[9−13] as well as to Zhong's and co-workers' recently-reported η values of 5.3−6.4% for various QD-functionalized TiO_2 electrodes prepared by linker-assisted assembly.[46−48] Our relatively low η values can be attributed primarily to low values of J_{sc} (Table 1), which were just 10−20% of those of the most efficient QDSSCs.

We calculated absorbed photon−current efficiencies under white-light illumination at short-circuit (APCE$_{WL}$) from average J_{sc} values of QDSSCs, absorptance spectra of CdSe-functionalized TiO_2 films, and the irradiance spectrum of our white-light source, using calculations described previously.[28] Data are summarized in Table 1. The average integrated absorbed photon flux ($q_{p,abs}$) (under illumination by our white-light source) of RQD-functionalized TiO_2 films was (46 ± 13)% greater than that of MSC-functionalized TiO_2 films; therefore, RQDs harvest white light more efficiently than MSCs, due to their red-shifted absorption spectra. Average values of APCE$_{WL}$ for QDSSCs incorporating RQD- and MSC-functionalized TiO_2 were 0.32 ± 0.03 and 0.29 ± 0.03, respectively. APCE$_{WL}$ for MSC/RQD-functionalized TiO_2 electrodes was (27 ± 16)% less than that of RQD-functionalized TiO_2. APCE equals the product of the electron-injection yield (ϕ_{inj}) and charge-collection efficiency (η_{el}).[51] Thus, poor values of ϕ_{inj} and/or η_{el} contributed to the low J_{sc} of our QDSSCs relative to the most efficient reported QDSSCs. Values of APCE$_{WL}$ for each of our CdSe samples were similar to the monochromatic APCEs from photocurrent action spectra (Figure S2 in the Supporting Information), indicating that ϕ_{inj} and η_{el} were essentially wavelength-independent. Importantly, the similarity of APCE$_{WL}$ values for QDSSCs with MSC- and RQD-functionalized TiO_2 electrodes implies that ϕ_{inj} and η_{el} were insensitive to the significant differences in the electronic properties of these CdSe QDs.

CONCLUSIONS

We synthesized water-dispersible cysteinate(2$^-$)-capped RQDs with lower-energy absorption onsets and excitonic absorption maxima than the previously-reported CdSe MSCs, simply by heating reaction mixtures to promote particle growth. The resulting CdSe RQDs adsorbed readily to bare nanocrystalline TiO_2 films through a single surface-attachment reaction. Excitonic absorption bands of the RQDs were unperturbed upon immobilization on surfaces. One goal of this study was to determine whether our previously-reported increases of ϕ_{inj}, charge-separated-state lifetime, APCE, and η, for cysteinate-(2$^-$)-capped CdSe MSCs, relative to CdSe RQDs capped with non-aminated linkers, were associated with properties of cysteinate(2$^-$), such as its surface dipole or the role of its amine as a ligand, or of MSCs, such as their high-energy excitonic and trap states. Values of η, monochromatic APCE, and APCE$_{WL}$ for our QDSSCs incorporating cysteinate(2$^-$)-capped CdSe RQDs were similar to or exceeded those of QDSSCs incorporating cysteinate(2$^-$)-capped CdSe MSCs; therefore, the favorable interfacial charge-transfer reactivity is not unique to MSCs and can instead be attributed to properties of cysteinate(2$^-$). This fortunate result suggests that cysteinate-(2$^-$) may be used to promote interfacial charge transfer in a range of systems.

In summary, the synthesis and linker-assisted assembly chemistry reported in this article represent a simple and all-aqueous method for functionalizing TiO_2 with presynthesized QDs having broadly tunable light-harvesting properties and desirable electron-injection reactivity for sensitization and energy conversion.

ASSOCIATED CONTENT

Supporting Information

Photoelectrochemical data: monochromatic APCE spectra for QDSSCs and short-circuit photocurrent action spectra and $J-V$ data for N3-sensitized solar cells. This material is available free of charge via the Internet at http://pubs.acs.org.

AUTHOR INFORMATION

Corresponding Author

*E-mail: dwatson3@buffalo.edu.

Notes

The authors declare no competing financial interest.

ACKNOWLEDGMENTS

This work was supported by the National Science Foundation (CHE-0645678).

REFERENCES

(1) Hodes, G. *J. Phys. Chem. C* **2008**, *112*, 17778−17787.
(2) Kamat, P. V. *J. Phys. Chem. C* **2008**, *112*, 18737−18753.
(3) Beard, M. C. *J. Phys. Chem. Lett.* **2011**, *2*, 1282−1288.
(4) Beard, M. C.; Luther, J. M.; Semonin, O. E.; Nozik, A. J. *Acc. Chem. Res.* **2013**, *46*, 1252−1260.
(5) Rühle, S.; Shalom, M.; Zaban, A. *ChemPhysChem* **2010**, *11*, 2290−2304.
(6) Kamat, P. V. *Acc. Chem. Res.* **2012**, *45*, 1906−1915.

(7) Mora-Seró, I.; Bisquert, J. *J. Phys. Chem. Lett.* **2010**, *1*, 3046−3052.
(8) Sambur, J. B.; Novet, T.; Parkinson, B. A. *Science* **2010**, *330*, 63−66.
(9) Lee, Y.-L.; Lo, Y.-S. *Adv. Funct. Mater.* **2009**, *19*, 604−609.
(10) González-Pedro, V.; Xu, X.; Mora-Seró, I.; Bisquert, J. *ACS Nano* **2010**, *4*, 5783−5790.
(11) Chang, J. A.; Rhee, J. H.; Im, S. H.; Lee, Y. H.; Kim, H.-j.; Seok, S. I.; Nazeeruddin, M. K.; Grätzel, M. *Nano Lett.* **2010**, *10*, 2609−2612.
(12) Santra, P. K.; Kamat, P. V. *J. Am. Chem. Soc.* **2012**, *134*, 2508−2511.
(13) Seol, M.; Kim, H.; Tak, Y.; Yong, K. *Chem. Commun.* **2010**, *46*, 5521−5523.
(14) Watson, D. F. *J. Phys. Chem. Lett.* **2010**, *1*, 2299−2309.
(15) Sambur, J. B.; Riha, S. C.; Choi, D.; Parkinson, B. A. *Langmuir* **2010**, *26*, 4839−4847.
(16) Hyun, B.-R.; Zhong, Y.-W.; Bartnik, A. C.; Sun, L.; Abruña, H. D.; Wise, F. W.; Goodreau, J. D.; Matthews, J. R.; Leslie, T. M.; Borrelli, N. F. *ACS Nano* **2008**, *2*, 2206−2212.
(17) Guijarro, N.; Lana-Villarreal, T.; Mora-Seró, I.; Gómez, R. *J. Phys. Chem. C* **2009**, *113*, 4208−4214.
(18) Giménez, S.; Mora-Seró, I.; Macor, L.; Guijarro, N.; Lana-Villarreal, T.; Gómez, R.; Diguna, L. J.; Shen, Q.; Toyoda, T.; Bisquert, J. *Nanotechnology* **2009**, *20*, 295204.
(19) Guijarro, N.; Shen, Q.; Giménez, S.; Mora-Seró, I.; Bisquert, J.; Lana-Villarreal, T.; Toyoda, T.; Gómez, R. *J. Phys. Chem. C* **2010**, *114*, 22352−22360.
(20) Pernik, D. R.; Tvrdy, K.; Radich, J. G.; Kamat, P. V. *J. Phys. Chem. C* **2011**, *115*, 13511−13519.
(21) King, L. A.; Riley, D. J. *J. Phys. Chem. C* **2012**, *116*, 3349−3355.
(22) Kern, M. E.; Watson, D. F. *Langmuir* **2012**, *28*, 15598−15605.
(23) Robel, I.; Subramanian, V.; Kuno, M.; Kamat, P. V. *J. Am. Chem. Soc.* **2006**, *128*, 2385−2393.
(24) Dibbell, R. S.; Watson, D. F. *J. Phys. Chem. C* **2009**, *113*, 3139−3149.
(25) Dibbell, R. S.; Youker, D. G.; Watson, D. F. *J. Phys. Chem. C* **2009**, *25*, 18643−18651.
(26) Mora-Seró, I.; Giménez, S.; Moehl, T.; Fabregat-Santiago, F.; Lana-Villarreal, T.; Gómez, R.; Bisquert, J. *Nanotechnology* **2008**, *19*, 424007.
(27) Margraf, J. T.; Ruland, A.; Sgobba, V.; Guldi, D. M.; Clark, T. *Langmuir* **2013**, *29*, 2434−2438.
(28) Nevins, J. S.; Coughlin, K. M.; Watson, D. F. *ACS Appl. Mater. Interfaces* **2011**, *3*, 4242−4253.
(29) Park, Y.-S.; Dmytruk, A.; Dmitruk, I.; Yasuto, N.; Kasuya, A.; Takeda, M.; Ohuchi, N. *J. Nanosci. Nanotechol.* **2007**, *7*, 3750−3753.
(30) Park, Y.-S.; Dmytruk, A.; Dmitruk, I.; Kasuya, A.; Takeda, M.; Ohuchi, N.; Okamoto, Y.; Kaji, N.; Tokeshi, M.; Baba, Y. *ACS Nano* **2010**, *4*, 121−128.
(31) Baker, J. S.; Nevins, J. S.; Coughlin, K. M.; Colón, L. A.; Watson, D. F. *Chem. Mater.* **2011**, *23*, 3546−3555.
(32) Dibbell, R. S.; Soja, G. R.; Hoth, R. M.; Watson, D. F. *Langmuir* **2007**, *23*, 3432−3439.
(33) Mann, J. R.; Watson, D. F. *Langmuir* **2007**, *23*, 10924−10928.
(34) Tachibana, Y.; Umekita, K.; Otsuka, Y.; Kuwabata, S. *J. Phys. D: Appl. Phys.* **2008**, *41*, 102002.
(35) Mann, J. R.; Gannon, M. K.; Fitzgibbons, T. C.; Detty, M. R.; Watson, D. F. *J. Phys. Chem. C* **2008**, *112*, 13057−13061.
(36) Nazeeruddin, M. K.; Kay, A.; Rodicio, I.; Humphry-Baker, R.; Müller, E.; Liska, P.; Vlachopoulos, N.; Grätzel, M. *J. Am. Chem. Soc.* **1993**, *115*, 6382−6390.
(37) Tachan, Z.; Shalom, M.; Hod, I.; Rühle, S.; Tirosh, S.; Zaban, A. *J. Phys. Chem. C* **2011**, *115*, 6162−6166.
(38) Murray, C. B.; Norris, D. J.; Bawendi, M. G. *J. Am. Chem. Soc.* **1993**, *115*, 8706−8715.
(39) Bowen Katari, J. E.; Colvin, V. L.; Alivisatos, A. P. *J. Phys. Chem.* **1994**, *98*, 4109−4117.
(40) Yu, W. W.; Qu, L.; Guo, W.; Peng, X. *Chem. Mater.* **2003**, *15*, 2854−2860.
(41) Yu, K. *Adv. Mater.* **2012**, *24*, 1123−1132.
(42) Park, Y.-S.; Dmytruk, A.; Dmitruk, I.; Kasuya, A.; Okamoto, Y.; Kaji, N.; Tokeshi, M.; Baba, Y. *J. Phys. Chem. C* **2010**, *114*, 18834−18840.
(43) Nazeeruddin, M. K.; Péchy, P.; Renouard, T.; Zakeeruddin, S. M.; Humphry-Baker, R.; Comte, P.; Liska, P.; Cevey, L.; Costa, E.; Shklover, V.; Spiccia, L.; Deacon, G. B.; Bignozzi, C.; Grätzel, M. *J. Am. Chem. Soc.* **2001**, *123*, 1613−1624.
(44) Chakrapani, V.; Baker, D.; Kamat, P. V. *J. Am. Chem. Soc.* **2011**, *133*, 9607−9615.
(45) Chen, J.; Zhao, D. W.; Song, J. L.; Sun, X. W.; Deng, W. Q.; Liu, X. W.; Lei, W. *Electrochem. Commun.* **2009**, *11*, 2265−2267.
(46) Zhang, H.; Cheng, K.; Hou, Y. M.; Fang, Z.; Pan, Z. X.; Wu, J. L.; Zhong, X. H. *Chem. Commun.* **2012**, *48*, 11235−11237.
(47) Pan, Z.; Huang, H.; Cheng, K.; Hou, Y.; Hua, J.; Zhong, X. *ACS Nano* **2012**, *6*, 3982−3991.
(48) Pan, Z.; Zhao, K.; Wang, J.; Zhang, H.; Feng, Y.; Zhong, X. *ACS Nano* **2013**, *7*, 5215−5222.
(49) Yella, A.; Lee, H.-W.; Tsao, H. N.; Yi, C.; Chandiran, A. K.; Nazeeruddin, M. K.; Diau, E. W.-G.; Yeh, C.-Y.; Zakeeruddin, S. M.; Grätzel, M. *Science* **2011**, *334*, 629−634.
(50) Yang, Z.; Chen, C.-Y.; Liu, C.-W.; Chang, H.-T. *Chem. Commun.* **2010**, *46*, 5485−5487.
(51) Watson, D. F.; Meyer, G. J. *Annu. Rev. Phys. Chem.* **2005**, *56*, 119−156.